Virginia Commonwealth University
VCU Scholars Compass

Electrical and Computer Engineering Publications | Dept. of Electrical and Computer Engineering

2006

Defect reduction in (112¯0) a-plane GaN by two-stage epitaxial lateral overgrowth

X. Ni
Virginia Commonwealth University, nix@vcu.edu

Ü. Özgür
Virginia Commonwealth University, uozgur@vcu.edu

Y. Fu
Virginia Commonwealth University

See next page for additional authors

Follow this and additional works at: http://scholarscompass.vcu.edu/egre_pubs

 Part of the Electrical and Computer Engineering Commons

Ni, X., Özgür, Ü., Fu, Y., et al. Defect reduction in (112¯0) a-plane GaN by two-stage epitaxial lateral overgrowth. Applied Physics Letters, 89, 262105 (2006). Copyright © 2006 AIP Publishing LLC.

Downloaded from
http://scholarscompass.vcu.edu/egre_pubs/106

This Article is brought to you for free and open access by the Dept. of Electrical and Computer Engineering at VCU Scholars Compass. It has been accepted for inclusion in Electrical and Computer Engineering Publications by an authorized administrator of VCU Scholars Compass. For more information, please contact libcompass@vcu.edu.

Authors
X. Ni, Ü. Özgür, Y. Fu, N. Biyikli, J. Xie, A. A. Baski, Hadis Morkoç, and Z. Liliental-Weber

This article is available at VCU Scholars Compass: http://scholarscompass.vcu.edu/egre_pubs/106

Defect reduction in $(11\bar{2}0)$ *a*-plane GaN by two-stage epitaxial lateral overgrowth

X. Ni,[a] Ü. Özgür, Y. Fu, N. Biyikli, J. Xie, A. A. Baski, and H. Morkoç
Department of Electrical and Computer Engineering, Virginia Commonwealth University, Richmond, Virginia 23284 and Department of Physics, Virginia Commonwealth University, Richmond, Virginia 23284

Z. Liliental-Weber
Lawrence Berkeley National Laboratory, Berkeley, California 94720

(Received 28 September 2006; accepted 20 November 2006; published online 26 December 2006)

The authors report a two-stage epitaxial lateral overgrowth (ELO) method to get uniformly coalesced $(11\bar{2}0)$ *a*-plane GaN using metal organic chemical vapor deposition by employing a relatively lower growth temperature in the first stage followed by conditions leading to enhanced lateral growth in the second. Using a two-stage ELO method the average Ga-polar to N-polar wing growth rate ratio has been reduced from 4–6 to 1.5–2, which consequently reduced the height difference between the two approaching wings at the coalescence front that resulted from the wing tilt (0.44° for Ga and 0.37° for N wings, measured by x-ray diffraction), thereby making their coalescence much easier. Transmission electron microscopy showed that the threading dislocation density in the wing areas was 1.0×10^{8} cm^{-2}, more than two orders of magnitude lower than that in the window areas (4.2×10^{10} cm^{-2}). However, high density of basal stacking faults of 1.2×10^{4} cm^{-1} was still present in the wing areas as compared to *c*-plane GaN where they are rarely observed away from the substrate. Atomic force microscopy and photoluminescence measurements on the coalesced ELO *a*-plane GaN sample also indicated improved material quality. © *2006 American Institute of Physics*. [DOI: 10.1063/1.2423328]

In *c*-axis-oriented hexagonal GaN system, the spontaneous and strain-induced piezoelectric polarizations produce strong electric fields that cause spatial separation of electrons and holes in quantum wells that are used for active regions in light emitters. Such a separation increases the recombination time[1] at the expense of the quantum efficiency[2] and also results in a redshift of the emission, the amount of which depends on the injected carrier density and the intentional doping due to screening. In short, additional constraints are placed on the design rules in an effort to deal with polarization-induced field. One approach to overcome this problem is to employ nonpolar *a*-plane hexagonal GaN, which can be grown on *r*-plane sapphire by, e.g., using metal organic chemical vapor deposition (MOCVD).[3–5] Investigations on *a*-plane AlGaN/GaN quantum wells[6–9] and light emitting diodes[10] have confirmed the absence of polarization-induced electric field. In order to realize high-performance nitride devices, epitaxial lateral overgrowth (ELO) by MOCVD could be used to reduce the density of threading dislocations (TDs) in *a*-plane GaN.[11,12] However, one cannot overlook the wing tilt, which has been shown to introduce some complexity at the coalescence boundaries even for *c*-plane GaN ELO.[13] In this letter, we report on the structural and optical characterization of *a*-plane GaN ELO samples grown by a two-stage MOCVD method to address the coalescence issue introduced by wing tilt.

The $(11\bar{2}0)$ *a*-plane GaN films were grown on $(1\bar{1}02)$ *r*-plane sapphire substrates.[5] A 1.5 μm thick *a*-plane GaN film with a low temperature GaN nucleation layer was used as the ELO template. An approximately 100 nm thick SiO_2 layer was grown on the *a*-plane GaN template by remote plasma enhanced chemical vapor deposition. Using conventional photolithography and buffer oxide etch, a striped mask pattern was transferred to SiO_2. The pattern consisted of 4 μm wide open windows and 20 or 10 μm wide SiO_2 stripes that were oriented along the $[1\bar{1}00]$ direction of GaN that would cause the lateral growth fronts to advance along the c^+ and c^- directions. The patterned template was then reloaded into the MOCVD chamber for overgrowth. Two *a*-GaN ELO samples were investigated for this particular study, samples A and B, grown with trimethylgallium and NH_3 flow rates of 157 μmol/min and 3000 SCCM (sccm denotes cubic centimeter per minute at STP), respectively. Sample A was grown in a single stage at 1050 °C for 3 h while sample B was grown in two stages: at 1000 °C for 2 h in stage I and at 1050 °C for 3 h in stage II. Each growth experiment was carried out on templates containing 10 and 20 μm wide SiO_2 stripes placed side by side in the growth chamber. The as-grown samples were characterized by scanning electron microscopy (SEM), atomic force microscopy (AFM), x-ray diffraction (XRD), transmission electron microscopy (TEM), and low temperature photoluminescence (PL). For a better view of the overgrown layer dimensions, the cross-sectional SEM measurements were performed on the 20 μm stripe samples, while the rest of the analysis was focused on the 10 μm stripe samples.

Figure 1(a) shows the plan-view SEM image of sample A after 0.5 h of overgrowth, where the *a*-plane GaN stripes were straight with (0001) and $(000\bar{1})$ side walls and no other facets were visible. The surface of sample A was fully coalesced after a total of 3 h of growth but with striations along and steps perpendicular to the *c* axis [see Fig. 1(b)]. As observed from the cross-sectional SEM image of Fig. 1(c), wings with Ga polarity were four to six times wider than those with N polarity, as also verified by TEM measure-

[a]Author to whom correspondence should be addressed; electronic mail: nix@vcu.edu

This article is copyrighted as indicated in the article. Reuse of AIP content is subject to the terms at: http://scitation.aip.org/termsconditions. Downloaded to IP: 128.172.48.58 On: Fri, 10 Apr 2015 18:22:15

 © 2006 American Institute of Physics

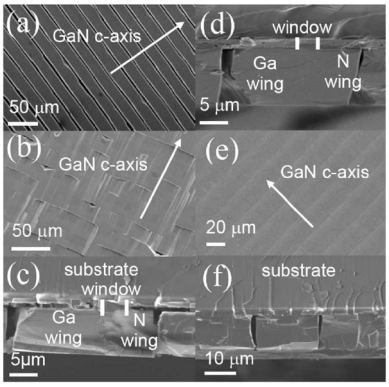

FIG. 1. Plan-view SEM images for sample A after (a) 0.5 h and (b) 3.0 h of growth. (c) Cross-sectional SEM image for sample A after 3 h of growth. (d) Cross-sectional SEM image for sample B after 2 h of growth at 1000 °C. (e) Plan-view and (f) cross-sectional SEM images for sample B, after a total of 5 h of growth.

ments. From the Kikuchi lines using large angle convergent beam electron diffraction (LACBED), a tilt angle of 0.25° and a twist (0.09°) between the two opposing wings were observed. As a consequence of the inherent wing tilt and largely different growth rates of the opposing wings, a clear height difference appears at the coalescence front. This height difference causes a significant surface undulation in *a*-plane GaN, in addition to defects, and is the origin of steps observed in Fig. 1(b). In order to get uniform coalescence and smooth overall surface, this height difference should be decreased or even eliminated if possible by reducing the difference between the widths or growth rates of the two opposite wings.

Growth temperature is a highly effective parameter to control the difference in the growth rates of the Ga and N wings. Therefore, for sample B, a two-stage growth method was employed where a 1000 °C growth temperature was used in stage I to favor vertical growth while maintaining a relatively low lateral growth rate which is not drastically different for the Ga and N fronts at this temperature. Figure 1(d) shows the sidewalls of *a*-GaN stripes after the stage I growth. It is worth pointing out that a large portion of the lateral growth was established with no coalescence during stage I where the Ga- to N-polar wing width ratio is close to 1.5. In stage II, temperature was elevated to 1050 °C to enhance the lateral growth for complete coalescence. Figures 1(e) and 1(f) show the plan-view and cross-sectional SEM images, respectively, for sample B after full coalescence (~15 μm total thickness). The Ga-polar wing is only 1.5–2 times wider than the N-polar wing as opposed to 4–6 for the single stage growth case. During stage II growth, with the temperature elevated, the sidewalls became fairly vertical, and after coalescence voids formed beneath the meeting fronts due to the absence of reactive sources. These results indicate that the attempts to suppress the uneven average growth rates of Ga and N wings by enhancing the vertical growth rate in the early stage of the growth were successful, leading to reduced step height at the meeting fronts.

To determine the wing tilt angles, XRD rocking curve measurements (Philips X'Pert MRD) were carried out with three different ϕ angles, which are the angles of rotation about the sample surface normal and defined as 0° when the projection of incident x-ray beam is parallel to the SiO_2 mask stripes. As shown in Fig. 2, for ϕ=0°, only one diffraction peak from the *a* plane of GaN can be observed, with full widths at half maximum (FWHMs) of 0.40° and 0.19° for

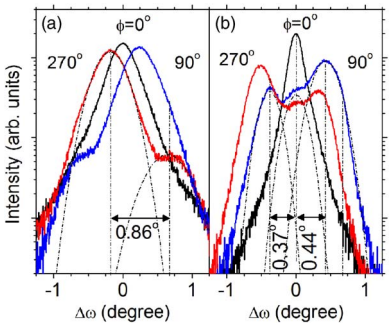

FIG. 2. (Color online) XRD ω-scan rocking curve data for (a) sample A and (b) sample B with different ϕ angles. The dashed lines in the figures correspond to the multiple Gaussian fits to the rocking curve data.

samples A and B, respectively. For ϕ=90° (x-ray beam is perpendicular to the mask stripes), however, samples A and B exhibit two and three peaks, respectively, the order of which is reversed for ϕ=270°. The strong peak observed for sample A is from the Ga-polar wings according to the XRD geometry used since the Ga-wing area is much larger than that of the N wing and the window as verified by SEM images discussed above. Therefore, the weak peak is assumed to be from the windows and/or N wings. The observed tilt angle of 0.86° is much larger than that obtained from the LACBED (0.25°). This variation may be attributed to the local nature of the LACBED measurement, while XRD provides a value averaged over a much larger area. In the case of sample B, smaller XRD linewidths in Fig. 2(b) compared to that for sample A indicate improved crystalline quality, and therefore, peaks from all three regions are distinguishable. The peak with the strongest intensity, shown in Fig. 2(b), is again from the Ga-polar wings (0.44° tilt), while the central one is from the crystal plane in the windows, and the third is from the N-polar wings (0.37° tilt). AFM measurements on both samples (not shown) showed elevated meeting fronts (~100 nm) after full coalescence due to the 1.05° miscut of the $(1\bar{1}02)$ *r*-plane sapphire towards its [0001] *c* axis obtained from XRD analysis. This miscut, which is larger than the tilt angles of both of the wings, resulted in the tilt of the GaN *a* plane and upward slope of the N wings with respect to the substrate surface, giving rise to the elevation at the meeting fronts.

TEM studies indicated a reduction of the TD density from 4.2×10^{10} cm^{-2} in the windows to 1.0×10^{8} cm^{-2} in the

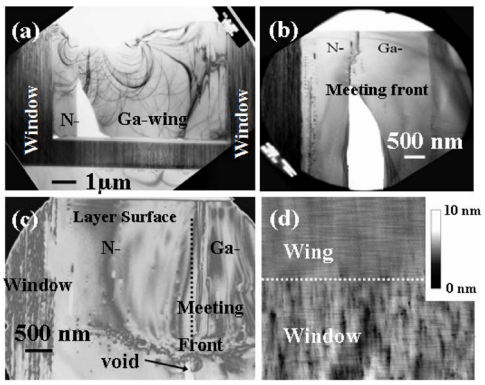

FIG. 3. Cross-sectional TEM images showing (a) the window and wing regions, and (b) the meeting front between Ga and N wings for sample A. (c) Cross-sectional TEM image for sample B. (d) 4×4 μm^2 AFM image near the window–N-wing boundary of sample B, showing different surface pit densities for the window and the wing.

This article is copyrighted as indicated in the article. Reuse of AIP content is subject to the terms at: http://scitation.aip.org/termsconditions. Downloaded to IP: 128.172.48.58 On: Fri, 10 Apr 2015 18:22:15

wings for sample A, which is clearly evidenced in Fig. 3(a). However, a relatively high density of basal stacking faults (BSFs), 1.2×10^4 cm^{-1}, was still observed in the wing areas compared to 1.3×10^6 cm^{-1} in the windows, which is not surprising considering their low formation energy of BSFs during a-*a*plane GaN growth.[14,15] It is more important to note that these stacking faults propagate to the sample surface, and therefore, may intersect any active area of the device grown on such layers, while in the case of *c*-plane GaN growth BSFs are formed only close to the substrate[16] and are rarely observed in the upper parts of the layers.[17] As shown in Fig. 3(b) dislocations were also found at the meeting fronts, as in the case of *c*-plane ELO.[18] Sample B also showed almost two orders of magnitude reduction of dislocations in the wings and generation of new dislocations at the meeting fronts [Fig. 3(c)]. When the neighboring wings coalesce, a grain boundary is formed on the prismatic plane with the shift vector parallel to [0001] [see Fig. 3(c)]. These boundaries sometimes eliminate BSFs propagating from the substrate, but often are the sources of new defects propagating to the surface.

To further characterize the surface topology of the films, tapping-mode AFM measurements were conducted which revealed significantly different densities of surface pits in the window and wing regions of the as grown samples which could be finger print of dislocation terminating at the surface.[19] Figure 3(d) shows an AFM image near the window–N-wing boundary for sample B, where the pit density in the windows ($\sim3.0\times10^9$ cm^{-2}) is approximately two orders of magnitude larger than that in the wings ($\sim3.7\times10^7$ cm^{-2}). TEM and AFM results therefore both confirm the effective dislocation reduction in *a*-plane ELO.

Optical properties of the films were probed by 15 K PL measurements performed on the overgrown GaN layers using 325 nm excitation from a HeCd laser. The near band edge emission (not shown) was composed of two peaks at 3.475 and 3.419 eV with FWHMs of 19 and 30 meV, respectively, where the former resulted from the free exciton and donor bound exciton transitions. The 3.419 eV peak has been attributed to the recombination of carriers/excitons bound to either stacking faults[20] or structural defects on the surface.[21] The band edge emission in sample B was around two orders of magnitude stronger than that in a control sample grown directly on sapphire under similar growth conditions but without the ELO process.

The origin for the different growth rates of Ga- and N-polar wings, which was also shown to exist during the lateral growth of *m*-plane GaN,[22] is not well established. Some authors tentatively attributed it to different adsorption or desorption rates on Ga and N faces.[12] However, our experiments show that under the same conditions, N-face and Ga-face *c*-plane GaN have similar growth rates, which was also verified by others.[23] Therefore, we speculate that this phenomenon may be related to differences in chemical stability of Ga and N faces since the latter has been shown to be less resistive to wet chemical etching.[24] During the growth of *a*-GaN, relatively lower amount of ammonia and higher growth temperature in hydrogen atmosphere may make N face even less stable than the Ga face, thereby inducing a smaller growth rate for the N-face GaN.

In conclusion, by employing a two-stage ELO of *a*-plane GaN with an initially enhanced vertical growth that was followed by enhanced lateral growth at an elevated temperature, the Ga- to N-wing width ratio and the wing height difference at the coalescence fronts have been reduced, resulting in a relatively flat fully coalesced surface. TEM studies indicated formation of a new boundary on inclined prismatic plane and dislocations along the vertical growth direction at the coalescence areas due to formation of step height between the two wings. In spite of this, the threading dislocation density was reduced from 4.2×10^{10} cm^{-2} in the window regions to 1.0×10^8 cm^{-2} in the wing regions, which still had a relatively high basal stacking fault density of 1.2×10^4 cm^{-1}. The improvement in the overgrown layer quality by ELO was also verified by AFM, which showed reduced surface pit density in the wings, and by PL in terms of increased intensity of the band edge emission.

This work in both laboratories was supported by the Air Force Office of Scientific Research under the direction of K. Reinhardt. The use of the NCEM facility in Berkeley is appreciated. Useful discussions with J. Leach, C. J. Moore, and V. P. Kasliwal are acknowledged.

[1] R. Langer, J. Simon, V. Ortiz, N. T. Pelekanos, A. Barski, R. Andre, and M. Godlewski, Appl. Phys. Lett. **74**, 3827 (1999).
[2] T. Deguchi, K. Sekiguchi, A. Nakamura, T. Sota, R. Matsuo, S. Chichibu, and S. Nakamura, Jpn. J. Appl. Phys., Part 2 **38**, L914 (1999).
[3] H. M. Ng, Appl. Phys. Lett. **80**, 4369 (2002).
[4] M. D. Craven, S. H. Lim, F. Wu, J. S. Speck, and S. P. DenBaars, Appl. Phys. Lett. **81**, 469 (2002).
[5] X. Ni, Y. Fu, Y. T. Moon, N. Biyikli, and H. Morkoç, J. Cryst. Growth **290**, 166 (2006).
[6] H. M. Ng, A. Bell, F. A. Ponce, and S. N. G. Chu, Appl. Phys. Lett. **83**, 653 (2003).
[7] T. Koida, S. F. Chichibu, T. Sota, M. D. Craven, B. A. Haskell, J. S. Speck, S. P. DenBaars, and S. Nakamura, Appl. Phys. Lett. **84**, 3768 (2004).
[8] H. Teisseyre, C. Skierbiszewski, B. Łucznik, G. Kamler, A. Feduniewicz, M. Siekacz, T. Suski, P. Perlin, I. Grzegory, and S. Porowski, Appl. Phys. Lett. **86**, 162112 (2005).
[9] S. Porowski, I. Grzegory, B. Łucznik, B. Pastuszka, M. Boćkowski, H. Teisseyre, Cz. Skierbiszewski, G. Kamler, G. Nowak, J. Smalc, and M. Kryśko, Proc. SPIE **6121**, 612107 (2006).
[10] A. Chitnis, C. Chen, V. Adivarahan, M. Shatalov, E. Kuokstis, V. Mandavilli, J. Yang, and M. A. Khan, Appl. Phys. Lett. **84**, 3663 (2004).
[11] M. D. Craven, S. H. Lim, F. Wu, J. S. Speck, and S. P. DenBaars, Appl. Phys. Lett. **81**, 1201 (2002).
[12] C. Chen, J. Yang, H. Wang, J. Zhang, V. Adivarahan, M. Gaevski, E. Kuokstis, Z. Gong, M. Su, and M. A. Khan, Jpn. J. Appl. Phys., Part 2 **42**, L640 (2003).
[13] P. Fini, H. Marchand, J. P. Ibbetson, S. P. DenBaars, U. K. Mishra, and J. S. Speck, J. Cryst. Growth **209**, 581 (2000).
[14] Z. Liliental-Weber, D. Zakharov, B. Wagner, and R. F. Davis, Proc. SPIE **6121**, 612101 (2005).
[15] D. Hull and D. J. Bacon, *Introduction to Dislocation* (Pergamon, Oxford, 1984), Chap. 6, p. 102.
[16] Z. Liliental-Weber and D. Cherns, J. Appl. Phys. **89**, 7833 (2001).
[17] F. A. Ponce, Mater. Res. Bull. **22**, 51 (1997).
[18] Z. Liliental-Weber, M. Benamara, W. Swider, J. Washburn, J. Park, P. A. Grudowski, C. J. Eiting, and R. D. Dupuis, MRS Internet J. Nitride Semicond. Res. **4S1**, G4.6 (2000).
[19] D. N. Zakharov, Z. Liliental-Weber, B. Wagner, Z. J. Reitmeier, E. A. Preble, and R. F. Davis, Phys. Rev. B **71**, 235334 (2005).
[20] P. P. Paskov, R. Schifano, T. Paskova, T. Malinauskas, J. P. Bergman, B. Monemar, S. Figge, and D. Hommel, Physica B **376–377**, 473 (2006).
[21] M. A. Reshchikov and H. Morkoç, J. Appl. Phys. **97**, 061301 (2005).
[22] B. A. Haskell, T. J. Baker, M. B. McLaurin, F. Wu, P. T. Fini, S. P. DenBaars, J. S. Speck, and S. Nakamura, Appl. Phys. Lett. **86**, 111917 (2005).
[23] R. Collazo, S. Mita, A. Aleksov, R. Schlesser, and Z. Sitar, J. Cryst. Growth **287**, 586 (2006).
[24] Y. Gao, M. D. Craven, J. S. Speck, S. P. DenBaars, and E. L. Hu, Appl. Phys. Lett. **84**, 3322 (2004).

This article is copyrighted as indicated in the article. Reuse of AIP content is subject to the terms at: http://scitation.aip.org/termsconditions. Downloaded to IP: 128.172.48.58 On: Fri, 10 Apr 2015 18:22:15